Main Group Chemistry

International Edition: DOI: 10.1002/anie.201504864
German Edition: DOI: 10.1002/ange.201504864

Six-Coordinate Group 13 Complexes: The Role of d Orbitals and Electron-Rich Multi-Center Bonding

Maarten G. Goesten, Célia Fonseca Guerra, Freek Kapteijn, Jorge Gascon, and F. Matthias Bickelhaupt**

In memory of Paul von Ragué Schleyer

Abstract: *Bonding in six-coordinate complexes based on Group 13 elements (B, Al, Ga, In, Tl) is usually considered to be identical to that in transition-metal analogues. We herein demonstrate through sophisticated electronic-structure analyses that the bonding in these Group 13 element complexes is fundamentally different and better characterized as electron-rich hypervalent bonding with essentially no role for the d orbitals. This characteristic is carried through to the molecular properties of the complex.*

Six-coordinate complexes based on Group 13 elements commonly occur in natural minerals, such as bayerite and böhmite, synthetic porous materials, such as metal–organic frameworks (MOFs), and soluble coordination compounds, for example, porphyrins.[1] The bonding in these systems is often treated as identical to that in transition-metal complexes, and numerous octahedral complexes indeed exist for both Group 13 elements and transition metals. The octahedral node in the MOF MIL-53 can be occupied by Sc^{3+}, Fe^{3+}, Cr^{3+}, Cu^{3+}, Al^{3+}, Ga^{3+} or In^{3+} (Figure 1), and it is the sporadic substitution of Al^{3+} by Cr^{3+} in an extended six-coordinate environment to which rubies owe their red color![2]

Nevertheless, it cannot be neglected that six-coordinate Group 13 complexes are formally hypervalent, and that their valence "breaks" the octet rule from a naïve point of view. Linus Pauling described hypervalence in terms of an expanded octet, in which low-energy d orbitals are invoked to account for extra bonding through hybridized sp^3d^2 orbitals.[3] This explanation would act as a bridge between the d and the p block and rationalize the apparent affinity towards comparable bonding topologies, but the expanded octet concept was convincingly dismissed by the seminal works of Rundle, Pimentel, Musher, von Ragué Schleyer, and Hiberty, who showed through both theory and computation that d orbitals lie too high in energy to significantly contribute to bonding in signature hypervalent molecules such as PF_5 and XeF_2, and that ionic configurations are rather dominant.[4]

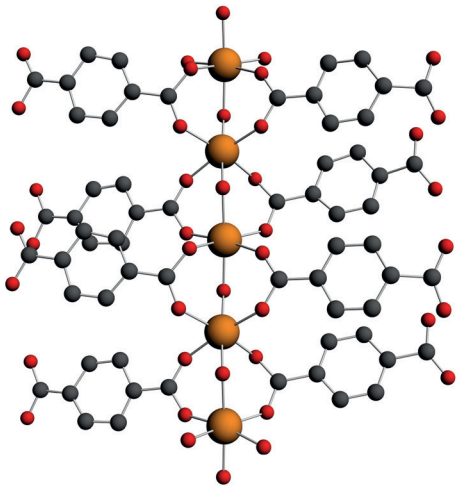

Figure 1. Octahedral nodes structuring the MIL-53 framework. The orange spheres represent six-coordinate M^{3+} ions (M = Sc, Fe, Cr, Cu, Al, Ga, In).

Considering these developments on the topic, as well as a recent spark of interest,[5] it is surprising that the rather common six-coordinate Group 13 based metal clusters have remained without sound theoretical treatment.

We herein examine the nature of the bonding in these systems for all non-radioactive Group 13 trications (B^{3+}, Al^{3+}, Ga^{3+}, In^{3+} and Tl^{3+}). These cations all have an empty valence shell in common and constitute ideal analogues of the transition-metal ion Sc^{3+}, with which their bonding is compared.

For O_h-symmetric Sc^{3+} complexes, a ligand field description with sp^3 lobes representing the ligand orbitals is expected to well describe bonding from a molecular orbital (MO) perspective (Figure 2 A). Here, six σ-bonding MOs originate from s–sp^3 (1), p–sp^3 (3), and d–sp^3 (2) metal–ligand overlap.

[*] M. G. Goesten, Prof. Dr. F. Kapteijn, Prof. Dr. J. Gascon
Catalysis Engineering, Delft University of Technology
Julianalaan 136, 2628BL Delft (The Netherlands)
M. G. Goesten
Inorganic Materials Chemistry, Eindhoven University of Technology
P.O.Box 513, 5600 MB Eindhoven (The Netherlands)
E-mail: M.G.Goesten@tue.nl
Dr. C. Fonseca Guerra, Prof. Dr. F. M. Bickelhaupt
Department of Theoretical Chemistry
VU University Amsterdam
De Boelelaan 1083, 1081 HV Amsterdam (The Netherlands)
E-mail: F.M.Bickelhaupt@vu.nl
Prof. Dr. F. M. Bickelhaupt
Institute of Molecules and Materials
Radboud University Nijmegen
Heyendaalseweg 135, 6525 AJ Nijmegen (The Netherlands)

Supporting information for this article is available on the WWW under http://dx.doi.org/10.1002/anie.201504864.

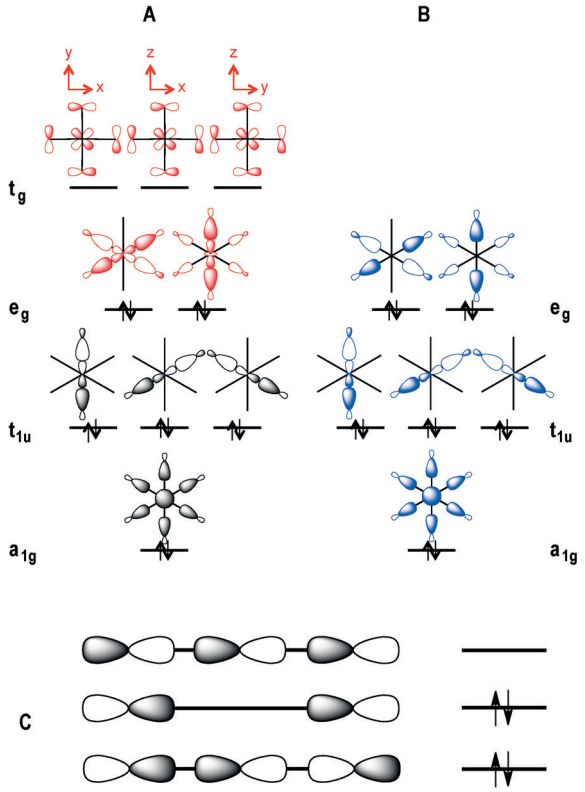

Figure 2. A) Schematic MO diagrams for an O_h-symmetric 12e complex with d orbitals (red). B) The same MO diagram without d orbitals (7c-12e pattern of MO bond order 4, blue). For A and B, the antibonding orbitals are omitted. C) The linear 3c-4e bond.

For an analogue based on a main-group element, the d orbitals are likely to be too high in energy to be involved in bonding, leading to an MO diagram similar to that of SF_6 (12-S-6; Figure 2B).[6]

The 7-center-12-electron (7c-12e) bonding pattern, shown in blue in Figure 2B, is the O_h analogue of the electron-rich, linear 3c-4e bond proposed by Rundle and Pimentel in the 1960s (Figure 2C).[4a,b] The qualitative MO bond orders are six and four for A and B, respectively, and thus 1 and $^2/_3$ per metal–ligand bond.

To answer the question as to whether bonding in the six-coordinate Group 13 complexes is better represented by scheme A or scheme B, we must examine the extent to which d orbitals are involved in the bonding mechanism and to what level they contribute to the structure and stability of the complexes.[5,7] To address these questions, we analyzed our model systems quantum-chemically using relativistic, dispersion-corrected density functional theory (DFT) at the ZORA-BLYP-D3(BJ)/TZ2P level of theory as implemented in the ADF program.[8]

First, we examined the importance of the various components of the bonding mechanism in terms of their contribution to the bond strength. This is done by decomposing the bonding energy between the M^{3+} fragment and the $(H_2O)_6$ fragment in the $[M(H_2O)_6]^{3+}$ complex of T_h symmetry, a subgroup of the O_h point group.[9] H_2O is our ligand of choice as we aimed to study a highly symmetric, yet realistic system. The bonding pattern associated with H_2O is expected to qualitatively carry through to the majority of systems in both solid-state and solution-state complexes.

The energy decomposition analysis (EDA) implemented in ADF breaks down the overall bond energy ΔE for the reaction $M^{3+} + 6\,H_2O \rightarrow [M(H_2O)_6]^{3+}$ into two major terms [Eq. (1)]:[10]

$$\Delta E = \Delta E_{prep} + \Delta E_{int} \quad (1)$$

ΔE_{prep} is the energy change associated with bringing six equilibrium-geometry H_2O molecules together into the $(H_2O)_6$ cage of ligands as it occurs in $[M(H_2O)_6]^{3+}$. ΔE_{int} represents the actual energy change when M^{3+} is combined with the prepared $(H_2O)_6$ fragment to form the final complex. ΔE_{int}, in turn, can be decomposed into classical electrostatic attractions, ΔV_{elstat}, the steric (Pauli) repulsion between closed shells, ΔE_{Pauli}, and orbital interactions, ΔE_{oi} [Eq. (2)]:[10]

$$\Delta E_{int} = \Delta V_{elstat} + \Delta E_{Pauli} + \Delta E_{oi} \quad (2)$$

The orbital-interaction term is of major interest as it is responsible for the various stabilizing donor–acceptor (e.g., HOMO–LUMO) interactions. It can be further decomposed into contributions from each irreducible representation [Eq. (3)]:

$$\Delta E_{oi} = \Delta E_s + \Delta E_p + \Delta E_{d\sigma} + \Delta E_{d\pi} \quad (3)$$

This furnishes a quantification of the donor–acceptor σ bonds involving the metal s AOs (ΔE_s in a_g symmetry), the three metal p AOs (ΔE_p in t_u), and the three metal d AOs ($\Delta E_{d\sigma}$ in e_g) as well as the donor–acceptor π bonds that involve the remaining metal d AOs ($\Delta E_{d\pi}$ in t_g). The data corresponding to the terms in Eq. (3) are graphically shown in Figure 3 (for full numerical details on these and all other energy terms occurring in Eq. (1)–(3), see the Supporting Information).

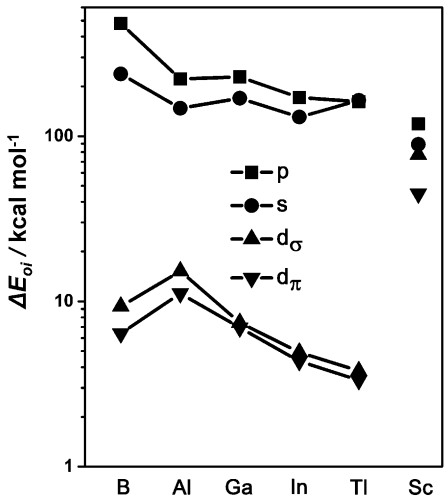

Figure 3. Bonding energy contributions of the s, p, and d orbitals in $[M(H_2O)_6]^{3+}$, M = B, Al, Ga, In, Tl, Sc.

Figure 3 clearly shows that the d orbital interactions do not make a significant contribution to the stability of the Group 13 metal complexes, as their interaction terms are an order of magnitude smaller than those of the s and p orbital interactions. This contrasts with the Sc^{3+} complex for which all orbital contributions are at comparable levels. Intriguingly, all Group 13 orbital trends display a kink at Al^{3+}, suggesting a slightly larger d orbital involvement for this particular case. This trend is also reflected by other quantitative measures of the bonding mechanism, such as the bond overlap and the fragment orbital population (see the Supporting Information).

Albeit in a subtle way, the above trend raises the question whether the central-atom d orbitals play a somewhat more significant role in determining the structure of the $[Al(H_2O)_6]^{3+}$ complex. To address this question, we carried out a numerical experiment in which the geometry of an initially distorted $[Al(H_2O)_6]^{3+}$ configuration was subjected to a geometry optimization using a basis set for aluminum from which all d functions had been deleted. The calculated metal–ligand bond length in the resulting $[Al(H_2O)]^{3+}$ complex turned out to be barely elongated at 195.7 pm, as compared to the value of 194.0 pm stemming from the computation where the aluminum d functions had been included. For example, this difference is considerably smaller than the one associated with the inclusion or exclusion of electron correlation: A geometry optimization at the Hartree–Fock/TZ2P level of theory resulted in a bond length of 199.7 pm.[11] We thus conclude that for the Group 13 based clusters, d orbitals are not part of the canonical description of the bonding, which is therefore represented by scheme B.

Next, we focused on the consequences of the above results for the electronic structure of $[M(H_2O)_6]^{3+}$ complexes based on Group 13 metals. The electron-rich, multi-center 7c-12e pattern predicts certain properties, such as 1) "elongated" metal–ligand bonds and 2) considerable charge polarization across these bonds.[6] In this context, "elongated" bonds refer to bonds that considerably exceed the bond length predicted by the sum of the covalent radii of the metal engaged in the interaction and an oxygen atom. Taking this as a measure, the six-coordinate clusters based on Group 13 cations are indeed held together by elongated bonds (Table 1). The six-coordinate scandium cluster, however, features metal–oxygen bonds that are shorter than the sum of the covalent radii. These values are consistent with the bonding and EDA analyses above and the formal MO bond orders of four and six. Nevertheless, it must be emphasized that these trends in bond length and formal bond order cannot be directly translated to bond strength as the total bond strength also depends on several other factors (e.g., orbital overlap, orbital energy gap) and features of the bonding mechanism (e.g., Pauli repulsion, electrostatic attraction). In fact, the average heterolytic M–O bond dissociation energy ($\langle BDE_{M-O}\rangle = (1/6)[E(M^{3+} + 6H_2O) - E([M(H_2O)_6]^{3+})]$ was computed to decrease from approximately 170 kcal mol^{-1} for the borium complex to 120–99 kcal mol^{-1} for the heavier Group 13 complexes and approximately 94 kcal mol^{-1} for the scandium complex.

Finally, we determined the charge distribution in our model systems by deformation density analysis, summarized on a per-atom basis using the Voronoi deformation density (VDD) method.[13] An increase in the metal radius leads to an increase in the local positive charge as the polarization ability of the cation diminishes (Figure 4). However, the charge polarization pattern across the M–O–H (M = metal) bond path is virtually equal between aluminum and scandium, even though their respective atomic van der Waals radii differ considerably (Al: 184 pm, Ga: 187 pm, In: 193 pm, Tl: 196 pm, Sc: 211 pm). This is a typical consequence of electron-rich bonding associated with hypervalent compounds, in which electrons in excess to the octet tend to largely reside on the ligands (see the $1e_g$ orbitals in Figure 2B).[5b–d]

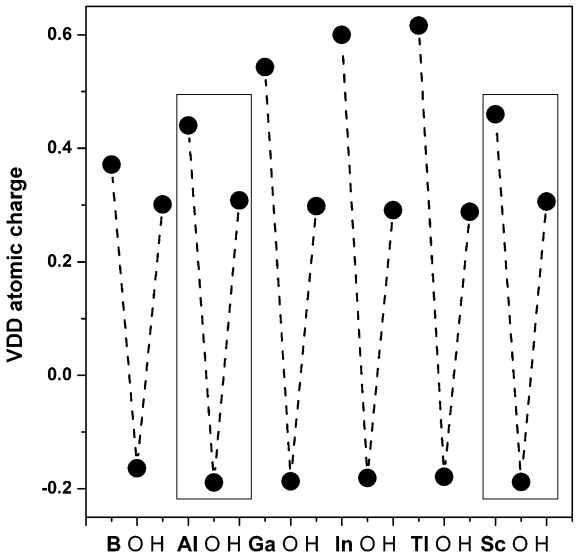

Figure 4. VDD atomic charges of the metal, oxygen, and hydrogen atoms in T_h $[M(H_2O)_6]^{3+}$ complexes. The charges for the aluminum and scandium hexaaqua complexes are shown in boxes.

Table 1: Sum of the metal and oxygen covalent radii and calculated bond lengths.

	B	Al	Ga	In	Tl	Sc
Sum of the covalent radii[a] [pm]	150 ± 5	187 ± 6	188 ± 5	208 ± 7	211 ± 9	233 ± 9
Bond length[b] [pm]	172.8	194.0	201.9	221.2	230.5	216.2

[a] From Ref. [12]. [b] Computed at the ZORA-BLYP-D3(BJ)/TZ2P level of theory.

In conclusion, we have shown that six-coordinate Group 13 based clusters are best conceived as electron-rich hypervalent species with highly polar 7-center-12-electron bonding. This is of direct explanatory value to some general features of materials based on these clusters, which are generally thermodynamically more stable, yet kinetically more reactive than their transition-metal-based analogues.[14] The insight obtained in this work will help chemists with the synthesis and characterization of new molecules and molecular frameworks, particularly those

targeting applications in luminescence, photocatalysis, and magnetism.

Experimental Section

Calculations: All standard calculations were performed with the Amsterdam Density Functional (ADF) program,[15] using the BLYP functional. The numerical integration was performed using the procedure developed by Boerrigter, te Velde, and Baerends.[16] The MOs were expanded in a large uncontracted set of Slater type orbitals (STOs) containing diffuse functions, which is of triple-ζ quality for all atoms and was augmented with two sets of polarization functions (TZ2P). The core shells of all atoms were treated by the frozen-core (FC) approximation.[17]

All energies and geometries were calculated using the generalized gradient approximation (GGA) of DFT at the BLYP level of theory.[18] GGA proceeds from the local density approximation (LDA) where exchange is described by Slater's X_α potential and correlation is treated in the Vosko–Wilk–Nusair (VWN) parametrization,[19] which is augmented with nonlocal corrections to exchange according to Becke,[18a] and correlations according to Perdew[20] added self-consistently.[21] For all calculations, relativistic effects were accounted for by the zeroth-order regular approximation (ZORA),[22] and dispersion was taken into account by Grimme's correction, D3.[23]

Additional geometry optimization calculations on $[Al(H_2O)_6]^{3+}$ were carried out using Hartree–Fock methods, and GGAs of DFT at the BLYP, OLYP,[24] and OPBE[25] levels of theory. All of these additional calculations were carried out at both TZ2P quality and quadruple-ζ quality with three polarization functions (QZ4P).

In the experiment on the role of the d orbitals on the geometry optimization, which is described in the main text, the d_{z^2}, $d_{x^2-y^2}$, d_{xy}, d_{xz}, and d_{yz} basis functions were deleted for the Al^{3+} fragment, after which the geometry optimization was performed on a complex of T_h symmetry with the initial O–Al bond length set to 210 pm.

Acknowledgements

We thank the Netherlands Organization for Scientific Research (NWO/CW) for financial support.

Keywords: bond theory · coordination modes · hypervalent compounds · main group chemistry · molecular orbital theory

How to cite: *Angew. Chem. Int. Ed.* **2015**, *54*, 12034–12038
Angew. Chem. **2015**, *127*, 12202–12206

[1] a) *Handbook of Mineralogy* (Eds.: J. W. Anthony, R. A. Bideaux, K. W. Bladh, M. C. Nichols), Mineralogical Society of America, Chantilly, VA, http://www.handbookofmineralogy.org; b) T. Devic, C. Serre, *Chem. Soc. Rev.* **2014**, *43*, 6097–6115; c) G. J. E. Davidson, L. H. Tong, P. R. Raithby, J. K. M. Sanders, *Chem. Commun.* **2006**, 3087–3089.

[2] a) F. Nouar et al., *Chem. Commun.* **2012**, *48*, 10237; b) C. Volkringer, T. Loiseau, N. Guillou, G. Férey, E. Elkaïm, A. Vimont, *Dalton Trans.* **2009**, 2241–2249; c) J. P. S. Mowat, V. R. Seymour, J. M. Griffin, S. P. Thompson, A. M. Z. Slawin, D. Fairen-Jimenez, T. Düren, S. E. Ashbrook, P. A. Wright, *Dalton Trans.* **2012**, *41*, 3937–3941; d) M. Anbia, S. Sheykhi, *J. Nat. Gas Chem.* **2012**, *21*, 680–684.

[3] S. J. French, *J. Chem. Educ.* **1940**, *17*, 551.

[4] a) R. J. Hach, R. E. Rundle, *J. Am. Chem. Soc.* **1951**, *73*, 4321–4324; b) G. C. Pimentel, *J. Chem. Phys.* **1951**, *19*, 446–448; c) J. I. Musher, *Angew. Chem. Int. Ed. Engl.* **1969**, *8*, 54–68; *Angew. Chem.* **1969**, *81*, 68–83; d) R. Hoffmann, J. M. Howell, E. L. Muetterties, *J. Am. Chem. Soc.* **1972**, *94*, 3047–3058; e) A. E. Reed, P. v. R. Schleyer, *J. Am. Chem. Soc.* **1990**, *112*, 1434–1445; f) F. M. Bickelhaupt, M. Solà, P. v. R. Schleyer, *J. Comput. Chem.* **1995**, *16*, 465–477; g) B. Braïda, P. C. Hiberty, *Nat. Chem.* **2013**, *5*, 417–422.

[5] a) S. C. A. H. Pierrefixe, S. J. M. van Stralen, J. N. P. van Stralen, C. Fonseca Guerra, F. M. Bickelhaupt, *Angew. Chem. Int. Ed.* **2009**, *48*, 6469–6471; *Angew. Chem.* **2009**, *121*, 6591–6593; b) S. C. A. H. Pierrefixe, C. Fonseca Guerra, F. M. Bickelhaupt, *Chem. Eur. J.* **2008**, *14*, 819–828; c) S. C. A. H. Pierrefixe, J. Poater, C. Im, F. M. Bickelhaupt, *Chem. Eur. J.* **2008**, *14*, 6901–6911; d) S. C. A. H. Pierrefixe, F. M. Bickelhaupt, *Struct. Chem.* **2007**, *18*, 813–819; e) W. C. McKee, J. Agarwal, H. F. Schaefer, P. v. R. Schleyer, *Angew. Chem. Int. Ed.* **2014**, *53*, 7875–7878; *Angew. Chem.* **2014**, *126*, 8009–8012; f) A. S. Ivanov, I. A. Popov, A. I. Boldyrev, V. V. Zhdankin, *Angew. Chem. Int. Ed.* **2014**, *53*, 9617–9621; *Angew. Chem.* **2014**, *126*, 9771–9775.

[6] K. Akiba, *Chemistry of hypervalent compounds*, Wiley, Hoboken, **1999**.

[7] E. Magnusson, *J. Am. Chem. Soc.* **1990**, *112*, 7940–7951.

[8] For ADF, see: a) www.scm.com; b) G. te Velde, F. M. Bickelhaupt, E. J. Baerends, C. Fonseca Guerra, S. J. A. van Gisbergen, J. G. Snijders, T. Ziegler, *J. Comput. Chem.* **2001**, *22*, 931–967; for BLYP, see: c) A. D. Becke, *Phys. Rev. A* **1988**, *38*, 3098–3100; d) C. Lee, W. Yang, R. G. Parr, *Phys. Rev. B* **1988**, *37*, 785–789; for ZORA, see: e) E. Van Lenthe, R. Van Leeuwen, E. J. Baerends, J. G. Snijders, *Int. J. Quantum Chem.* **1996**, *57*, 281–293; for DFT-D3, see: f) S. Grimme, J. Antony, S. Ehrlich, H. Krieg, *J. Chem. Phys.* **2010**, *132*, 154104.

[9] The T_h symmetry is the minimum on the potential energy surface for all cases except for $[Tl(H_2O)_6]^{3+}$, where the C_3 geometry is 0.91 kcal mol^{-1} lower in energy. For the sake of comparison between the metals in EDA, we used the T_h symmetry in our analysis. The coordinates for the C_3 complex are given in the Supporting Information.

[10] a) F. M. Bickelhaupt, E. J. Baerends in *Reviews in Computational Chemistry*, *Vol. 15* (Eds.: K. B. Lipkowitz, D. B. Boyd), Wiley-VCH, New York, **2000**, pp. 1–86; b) T. Ziegler, A. Rauk, *Inorg. Chem.* **1979**, *18*, 1755.

[11] We performed additional geometry optimizations, varying the GGA functional and basis set and monitoring the effect on the metal–ligand bond length for the Al^{3+} case. The results are (with all values given in pm): ZORA-BLYP-D3(BJ)/QZ4P: 195.2; ZORA-OPBE/TZ2P: 195; ZORA-OPBE/QZ4P: 195.2; ZORA-OLYP/TZ2P: 195.1; ZORA-OLYP/QZ4P: 195.8 (see Ref. [8a] and references cited therein). These values demonstrate that the change associated with removing the d functions does not exceed the spread in values associated with varying the functionals and basis sets in these high-level DFT approaches.

[12] B. Cordero, V. Gómez, A. E. Platero-Prats, M. Revés, J. Echeverría, E. Cremades, F. Barragán, S. Alvarez, *Dalton Trans.* **2008**, 2832.

[13] C. Fonseca Guerra, J.-W. Handgraaf, E. J. Baerends, F. M. Bickelhaupt, *J. Comput. Chem.* **2004**, *25*, 189–210.

[14] I. J. Kang, N. A. Khan, E. Haque, S. H. Jhung, *Chem. Eur. J.* **2011**, *17*, 6437–6442.

[15] a) www.scm.com; b) C. Fonseca Guerra, J. G. Snijders, G. te Velde, E. J. Baerends, *Theor. Chem. Acc.* **1998**, *99*, 391–403; see also Ref. [8b].

[16] a) P. M. Boerrigter, G. te Velde, J. E. Baerends, *Int. J. Quantum Chem.* **1988**, *33*, 87–113; b) G. te Velde, E. J. Baerends, *J. Comput. Phys.* **1992**, *99*, 84–98.

[17] E. J. Baerends, D. E. Ellis, P. Ros, *Chem. Phys.* **1973**, *2*, 41–51.

[18] See Ref. [8c,d].

[19] S. H. Vosko, L. Wilk, M. Nusair, *Can. J. Phys.* **1980**, *58*, 1200 – 1211.
[20] J. Perdew, *Phys. Rev. B* **1986**, *33*, 8822 – 8824.
[21] L. Fan, T. Ziegler, *J. Chem. Phys.* **1991**, *94*, 6057 – 6063.
[22] E. Van Lenthe, J. G. Snijders, E. J. Baerends, *J. Chem. Phys.* **1996**, *105*, 6505 – 6516; see also Ref. [8e].
[23] See Ref. [8f].
[24] N. C. Handy, A. J. Cohen, *Mol. Phys.* **2001**, *99*, 403 – 412.
[25] M. Swart, A. R. Groenhof, A. W. Ehlers, K. Lammertsma, *J. Phys. Chem. A* **2004**, *108*, 5479 – 5483.

Received: May 28, 2015
Revised: June 30, 2015
Published online: August 12, 2015

